

Article

Cold-Active Lipase-Based Biocatalysts for Silymarin Valorization through Biocatalytic Acylation of Silybin

Giulia Roxana Gheorghita ¹, Victoria Ioana Paun ², Simona Neagu ², Gabriel-Mihai Maria ², Madalin Enache ², Cristina Purcarea ², Vasile I. Parvulescu ¹ and Madalina Tudorache ^{1,*}

¹ Department of Organic Chemistry, Biochemistry and Catalysis, Faculty of Chemistry, University of Bucharest, 4-12 Regina Elisabeta Blvd., 030016 Bucharest, Romania; giulia.gheorghita@s.unibuc.ro (G.R.G.); vasile.parvulescu@chimie.unibuc.ro (V.I.P.)

² Department of Microbiology, Institute of Biology Bucharest, Romanian Academy, 296 Splaiul Independentei, 060031 Bucharest, Romania; ioana.paun@ibiol.ro (V.I.P.); simona.neagu@ibiol.ro (S.N.); gabriel.maria@ibiol.ro (G.-M.M.); madalin.enache@ibiol.ro (M.E.); cristina.purcarea@ibiol.ro (C.P.)

* Correspondence: madalina.sandulescu@g.unibuc.ro

Abstract: Extremophilic biocatalysts represent an enhanced solution in various industrial applications. Integrating enzymes with high catalytic potential at low temperatures into production schemes such as cold-pressed silymarin processing not only brings value to the silymarin recovery from biomass residues, but also improves its solubility properties for biocatalytic modification. Therefore, a cold-active lipase-mediated biocatalytic system has been developed for silybin acylation with methyl fatty acid esters based on the extracellular protein fractions produced by the psychrophilic bacterial strain *Psychrobacter SC65A.3* isolated from Scarisoara Ice Cave (Romania). The extracellular production of the lipase fraction was enhanced by 1% olive-oil-enriched culture media. Through multiple immobilization approaches of the cold-active putative lipases (using carbodiimide, aldehyde-hydrazine, or glutaraldehyde coupling), bio-composites (S1–5) with similar or even higher catalytic activity under cold-active conditions (25 °C) have been synthesized by covalent attachment to nano-/micro-sized magnetic or polymeric resin beads. Characterization methods (e.g., FTIR DRIFT, SEM, enzyme activity) strengthen the biocatalysts' settlement and potential. Thus, the developed immobilized biocatalysts exhibited between 80 and 128% recovery of the catalytic activity for protein loading in the range 90–99% and this led to an immobilization yield up to 89%. The biocatalytic acylation performance reached a maximum of 67% silybin conversion with methyl decanoate acylating agent and nano-support immobilized lipase biocatalyst.

Keywords: cold-active lipolytic activity; lipase immobilization; biocatalysis; silymarin; silybin



Citation: Gheorghita, G.R.; Paun, V.I.; Neagu, S.; Maria, G.-M.; Enache, M.; Purcarea, C.; Parvulescu, V.I.; Tudorache, M. Cold-Active Lipase-Based Biocatalysts for Silymarin Valorization through Biocatalytic Acylation of Silybin. *Catalysts* **2021**, *11*, 1390. <https://doi.org/10.3390/catal11111390>

Academic Editor: Gloria Fernandez-Lorente

Received: 24 October 2021

Accepted: 15 November 2021

Published: 17 November 2021

Publisher's Note: MDPI stays neutral with regard to jurisdictional claims in published maps and institutional affiliations.



Copyright: © 2021 by the authors. Licensee MDPI, Basel, Switzerland. This article is an open access article distributed under the terms and conditions of the Creative Commons Attribution (CC BY) license (<https://creativecommons.org/licenses/by/4.0/>).

1. Introduction

Silybum marianum is a very effective natural remedy known in the popular consciousness as milk thistle and originates from Southern and Southeastern Europe. Being associated with daisies and artichokes [1], *S. marianum* belongs to the aster family, *Asteraceae* or *Compositae*. From a biochemical point of view, *S. marianum* comprises a group of flavonolignans collectively known as the silymarin mixture. Milk thistle extract contains 30% to 65% silymarin: 20–45% silydianin, 40–65% silybin A and B, and 10–20% isosilybin A and B [2]. The flavonolignans from the extract are natural polyphenols, biogenetically related to lignans due to their similar synthetic pathways [3]. Two phenylpropanoid units linked to another complex structural part ensure the binding of the C₆C₃ ring with the flavonoid nucleus in different positions. These compounds show multiple chirality, which leads to the existence of several stereoisomers in nature [4,5].

The main component and the most biologically active of silymarin is silybin [6]. Structurally, the chromone ring of silybin is responsible for the weak acidic properties and the antioxidant response. It is given by the phenolic hydroxyls at 3,4- and 4,5- positions, which

form complexes with various metal ions [7]. Moreover, silybin exists in two stereoisomeric forms, A (2R, 3R, 10R, 11R) and B (2R, 3R, 10S, 11S), and has reduced solubility either in water or lipid media [8].

The cold-press silymarin extraction method proposed by Duran et al. is a more economical and energy efficient technique than either hot water extraction [9] or solvent-solvent partition [3,10]. The popularity of the cold-press method has increased since neither heat nor chemical treatment is used, and all beneficial nutritional properties of the raw material are transmitted to the oils. However, a problem arises in the light of the valorization of biomass waste, as silymarin abundantly passed into the residue [11]. Silymarin with anti-oxidative [12], anti-fibrotic, anti-inflammatory, membrane stabilizing, immunomodulatory, and liver regenerating properties plays an important role in experimental liver diseases [13]. There are also significant responses of flavonolignans to mushroom (*Amanita* sp.) poisoning, hepatitis, cirrhosis, and liver fibrosis [3], and the low water solubility of silymarin (430 mg/L) restricts therapeutic efficacy even if it is clinically safe at high doses (>1500 mg/day for humans) [14].

A new study on the bioavailability improvement was achieved through selective acylation of silybin in the 3-OH position with a 60% product yield in the presence of $\text{CeCl}_3 \cdot 7\text{H}_2\text{O}$ Lewis acid catalyst [8]. In order to obtain phosphorylated conjugates, Zarelli et al. initially acetylated silybin in a complex three-step organic synthetic process with a 75% yield [15]. Moreover, there are encapsulated silymarin variants in matrices less toxic and much better accepted by the human organism [10,16]. Silymarin could be included in natural β -cyclodextrins forming complexes, often used because of their solubilization potential within the body barriers without metabolic degradation [14]. Liposomal systems are known to find immediate access to reticulo-endothelial system (RES) rich sites like the liver and spleen, and this self-targeted nature of liposomal carriers can be exploited for silymarin distribution to hepatic sites [14,17].

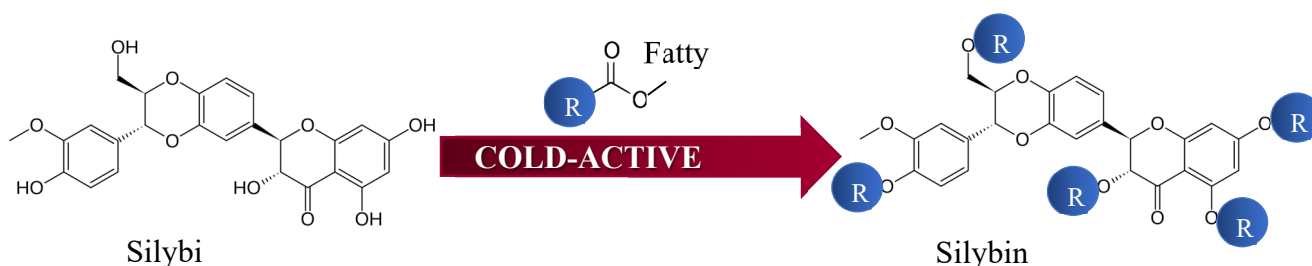
Besides chemical modification, or chemo-enzymatic or biocatalytic approaches, Xanthakis et al. showed that a lipase-based acylation of silybin with vinyl butyrate via Novozyme 435 biocatalyst strongly depends on the organic medium, where the conversion degree increased from 78 to 100% [18]. In favor of a faster synthesis, Vavrikova et al. used divinyl esters to modify silybin through *Candida antarctica* B lipase mediation and achieved silybin dimers with a 24–44% yield range [19].

Microorganisms inhabiting low-temperature environments including bacteria, yeasts, fungi, and algae [20] have adapted to produce cold-active enzymes that ensure the minimum rate of chemical and metabolic reactions [21,22]. The optimum temperatures for cold-adapted enzyme activities are usually in the range 20–30 °C, which could be considered close to that of the neutro-/thermophiles [21]. The ability of these enzymes to adjust their activity to low temperatures is based on their structural flexibility [23]. There are two strengths related to the active enzymes' operation: the manipulation of thermo-labile and sensitive substrates at low temperature and the inactivation of the enzyme when the temperature increases [20]. Few genomes of psychrophiles have been deposited in public databases [13].

Scarissoara Ice Cave is located in the Carpathian Mountains (Bihor, Romania) and has been accumulating perennial ice deposits for over 10,000 years. The constant negative temperatures throughout the year lead to a continuous deposit in glacial alternating organic-inorganic sediment layers. Thus, Scarissoara Ice Cave is known to host the world's oldest and largest underground perennial ice block [24]. During subsequent ice sampling from the Great Hall area of the cave, Paun et al. successfully determined the prokaryotic diversity [25] and isolated bacterial strains from a 13,000-year-old ice core [26]. The plethora of potentially active bacterial communities comprises 25 phyla, 58 classes, and 325 genera. Thus, a new *Psychrobacter* SC65A.3 was taxonomically assigned and characterized by C. Purcarea's research group (unpublished data).

For drug and cosmetic industries, a cold-active lipase-mediated system [27,28] for the acylation of silybin A/B with proper methyl fatty acid esters [29,30] has been designed to

improve the initial liposolubility [31,32] of silybin and to enhance silymarin bioavailability (Scheme 1).



Scheme 1. Acylation reaction of silybin with methyl fatty acid esters based on lipase biocatalysis.

In this context, the extracellular enzymatic fraction of the *Psychrobacter SC65A.3* strain recently isolated from the ice deposits of Scarisoara Ice Cave (Romania) was exploited for proper identification and characterization of the cold-active lipolytic activity. Therefore, new lipase-based biocatalysts were designed and used in a silybin conversion system at low temperature for silymarin valorization.

2. Results and Discussion

2.1. Evaluation of *Psychrobacter SC65A.3* Lipolytic Activity on Different Substrates

Formation of white calcium oleate microcrystals around the inoculum spot is a direct consequence of extracellular lipolytic activity, hence for the ability of the strain to hydrolyze the ester bond from a long hydrocarbon chain (C18, Tween 80). The diameter of the hydrolysis zone is directly proportional to the amount of enzymatic activity (Figure 1), so the larger the zone diameter, the more lipolytic activity. After seven days of 15 °C, the hydrolysis area expended near the reaction spot.

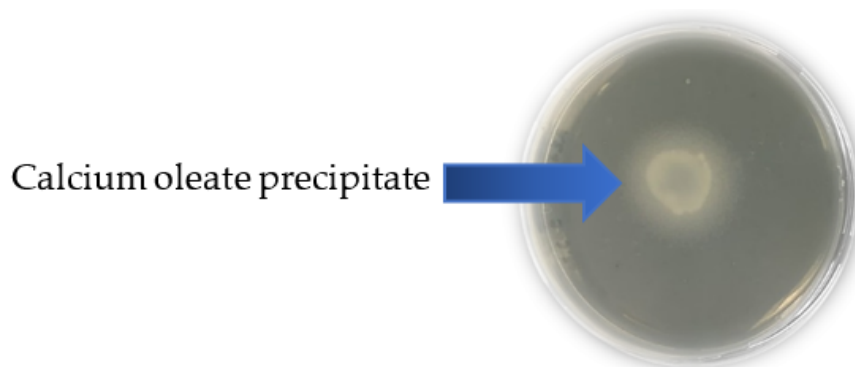


Figure 1. Lipolytic activity on Tween 80 substrate by formation of calcium oleate precipitate.

Screening on vegetable oils was performed to estimate the optimal substrate concentration that increases extracellular lipase production of *Psychrobacter SC65A.3*. The hydrolysate of oil substrate reacted with 0.001% Rhodamine B to create a red-orange, fluorescent halo under 350 nm UV light (Figure 2). However, the highest lipase activity for *Psychrobacter SC65A.3* was observed to be a concentration of 1% sunflower and 1% olive oil.

The *Psychrobacter SC65A.3* was cultivated at 15 °C for 3 days for fully grown cell colonies to produce and extracellularly release proteins into the culture medium supplemented with 1% olive oil, which is the preferred carbon source for lipolytic hydrolysis [33].

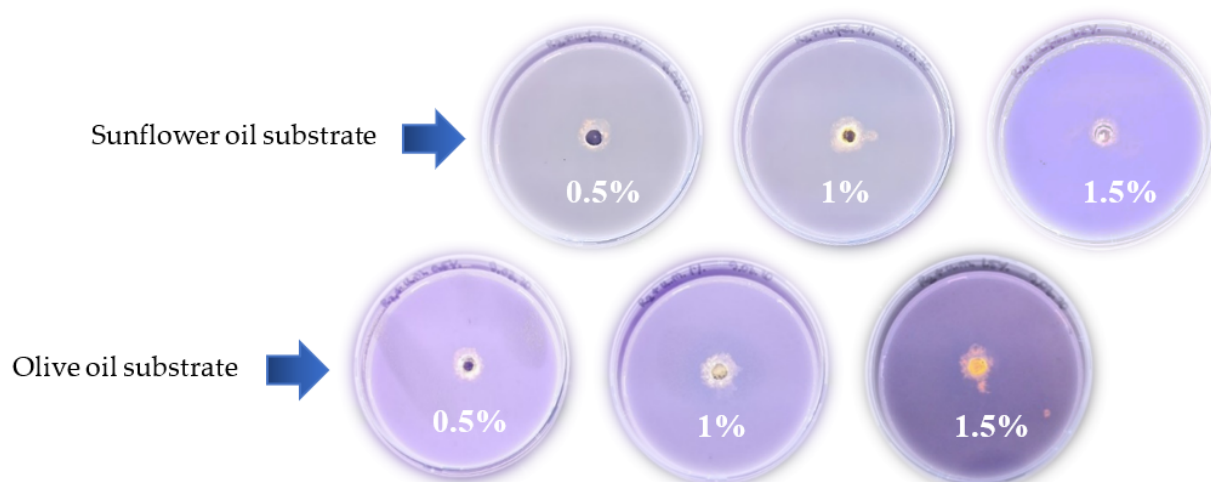


Figure 2. Lipolytic activity on vegetable oil substrates by formation of fluorescent complex.

2.2. Characterization of the Immobilized Cold-Active Lipase

Catalytic activity of cold-active lipase from the protein extracellular fraction was determined for both free and immobilized forms. A total of five bio-composites (S1–5) were prepared by covalent attachment of the protein extract on either magnetic particles or resin polymer supports using different immobilization approaches (see Section 3.). Protein loading of the bio-composites was calculated and the corresponding values are displayed in Table 1. Recovery of the lipase activity and also the immobilization yield were determined regarding the catalytic activity of the free lipase fraction ($4.4 \text{ U} \times \text{mg protein}^{-1}$). As a general remark, more than 95% protein loading was achieved for all the bio-composites with the immobilization yield in the range 74–89%. Additionally, the catalytic activity was preserved after the immobilization (around 80% recovery of the catalytic activity). A slight increase in the catalytic activity after immobilization ($105 \pm 5.1\%$ recovery of the catalytic activity) can be observed for the GA approach (S5), characterized by relatively good protein loading ($90 \pm 4.3\%$) and high immobilization yield ($89 \pm 4.0\%$). The lipase fraction underwent an “apparent” activation phenomenon, which is a common aspect of lipase behavior already reported in the literature [34]. In addition, the GA linker can exhibit a positive effect on the catalytic activity by placing the protein molecules away from the support surface to avoid the steric inhibition from protein–support interactions. Moreover, an increase in lipase activity was registered for the S2 bio-composite and can also be explained based on lipase “apparent” activation (see Table 1). In this case, the immobilization was performed based on the EDC approach, which led to high protein loading and significant immobilization yield. The greater availability of the support surface nano-design area for S2 allowed larger immobilization of the protein amount and avoided the steric inhibition by protein–protein interaction. Similarly, the periodate method exhibited good protein loading for low immobilization yield.

Table 1. Evaluation of the immobilization efficiency of the prepared bio-composites. (The experimental data were determined in triplicates).

	Recovery of Lipase Activity (%)	Immobilization Yield (%)	Protein Loading (%)
S1	82 ± 5.1	80 ± 4.5	99 ± 5.3
S2	128 ± 6.3	84 ± 4.7	99 ± 4.8
S3	80 ± 5.4	76 ± 4.3	93 ± 4.6
S4	82 ± 5.5	74 ± 4.8	96 ± 4.9
S5	105 ± 5.1	89 ± 4.0	90 ± 4.3

FTIR DRIFT analysis of free and immobilized lipase were performed. Interferograms of the supports were considered as the reference (Supplementary Material, Figure S1).

A simple comparison of the spectra confirmed the enzyme attachment to the support surface. For the immobilized specimens, the bands around $1550\text{--}1700\text{ cm}^{-1}$ specific for peptide bonds (Amide I and II region) [35] are recovered from the free biocatalyst. For S1–4, the bands in the range $570\text{--}650\text{ cm}^{-1}$ stand for Fe-O specific vibrations in the magnetic particles [36], while methacrylate support (S5) gives a particular band at 1730 cm^{-1} for the C=O stretching carboxyl, as well as two bands between 3300 and 3500 cm^{-1} for primary amino groups projecting out from the polymer outer face. Additionally, FTIR spectra allowed us to analyze the changes in protein secondary structure as a direct effect of the immobilization.

SEM characterization of the immobilized specimens is presented in Figure 3. As a method of control, SEM micrographs were obtained for purified lipase from *Aspergillus niger* (Supplementary Material, Figure S2). The protein aggregates dispersed freely in the liquid phase had similar profiles to the ones recovered from each support surface. Therefore, the protein content on the functionalized particle layer was highlighted. The aspect of magnetic particles is defined and characteristically crystallized to magnetite and maghemite (Figure 3). In the case of the free support based on methacrylate polymer, the beads have a clear, smooth surface. For immobilized lipase, changes in the morphology of the bio-composites occurred. A brighter contrast displays protein deposits that adhere covalently to the support surface [37,38]. In this way, the immobilization of the lipase on the solid support was confirmed one more time according to the results of FTIR analysis.

Kinetics measurements were performed for the immobilized lipase fraction and compared to a free lipase biocatalyst. The kinetic constants K_m and V_{max} , and particularly k_{cat} , were calculated for 25 and $37\text{ }^\circ\text{C}$ to confirm the cold-active behavior of the lipase. The corresponding values are presented in Table 2. Lipolytic activity of free and immobilized enzymes was detected for both tested temperatures (25 and $37\text{ }^\circ\text{C}$). According to the K_m values at $25\text{ }^\circ\text{C}$, lipase biocatalysts exhibited cold-active behavior, without substantial changes to the substrate's apparent affinity for a higher temperature ($37\text{ }^\circ\text{C}$). In the case of the catalytic constant (k_{cat}), similar values were recorded for both temperatures. For catalytic efficiency (k_{cat}/K_m), the close values for both temperatures support the structural and functional stability of the proteinaceous material.

Table 2. Kinetic parameters of cold-active lipase for both free and immobilized forms at $25\text{ }^\circ\text{C}$ and $37\text{ }^\circ\text{C}$, using $1/4\text{ v/v}$ lipase biocatalysts (see Section 3). (The experimental data were determined in triplicates.)

Biocatalyst	K_m (mM)		k_{cat} (min^{-1})		k_{cat}/K_m ($\text{mM}^{-1}\text{ min}^{-1}$)	
	$25\text{ }^\circ\text{C}$	$37\text{ }^\circ\text{C}$	$25\text{ }^\circ\text{C}$	$37\text{ }^\circ\text{C}$	$25\text{ }^\circ\text{C}$	$37\text{ }^\circ\text{C}$
Free	2.18 ± 0.15	1.85 ± 0.09	1.63 ± 0.08	1.95 ± 0.09	0.75 ± 0.05	1.05 ± 0.09
S1	1.61 ± 0.08	1.17 ± 0.09	0.99 ± 0.05	0.97 ± 0.06	0.62 ± 0.04	0.83 ± 0.04
S2	0.56 ± 0.04	0.65 ± 0.03	0.93 ± 0.05	0.99 ± 0.06	1.67 ± 0.09	1.54 ± 0.07
S3	4.18 ± 0.21	1.41 ± 0.07	2.29 ± 0.09	1.25 ± 0.07	0.55 ± 0.03	0.88 ± 0.04
S4	0.63 ± 0.03	0.78 ± 0.05	0.65 ± 0.03	0.92 ± 0.05	1.02 ± 0.09	1.17 ± 0.09
S5	0.94 ± 0.05	0.64 ± 0.03	0.85 ± 0.08	1.2 ± 0.09	0.90 ± 0.05	1.88 ± 0.09

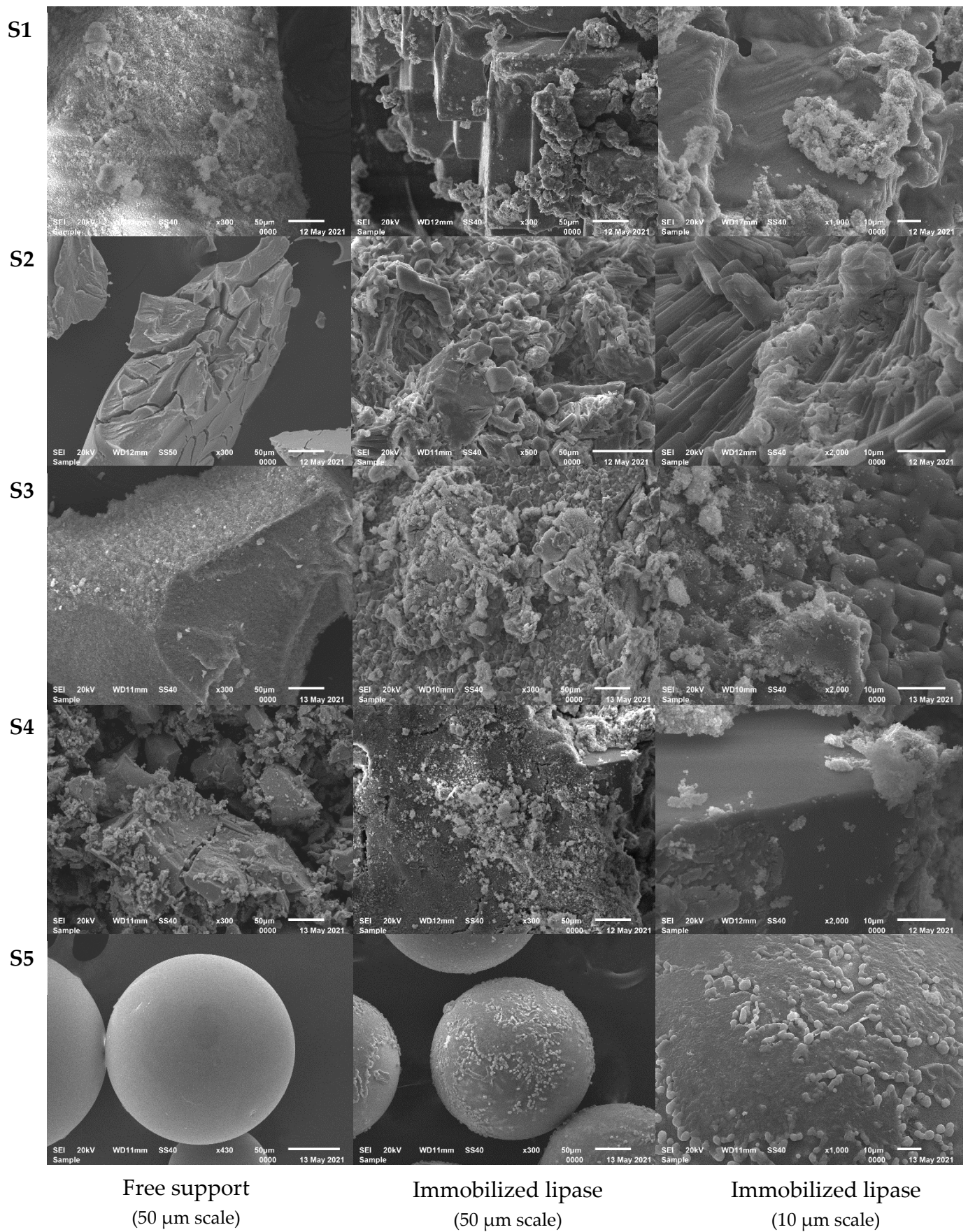


Figure 3. SEM micrographs of the bio-composites and corresponding supports.

2.3. Cold-Active Lipase Catalyzing Silybin Acylation

Free and immobilized cold-active lipase fractions were tested for the acylation of silybin substrate. Methyl fatty acid esters as acylating donors were used for the transesterification process that leads to silybin ester products (Scheme 1). The experiments were performed at 25 °C in line with the cold-active behavior of the expressed lipase. Additionally, the same enzymatic system was tested at 40 °C for comparison. For both temperatures, silybin was acylated with different acylation reagents (e.g., methyl decanoate, methyl laurate, methyl myristate, and methyl palmitate) and the reaction system was assisted by free lipase and S5 biocatalyst. THF was chosen as the organic solvent of the system (the activity of the cold-active lipase fraction was not affected by the THF—data are not included). The experimental results are presented in Figure 4.

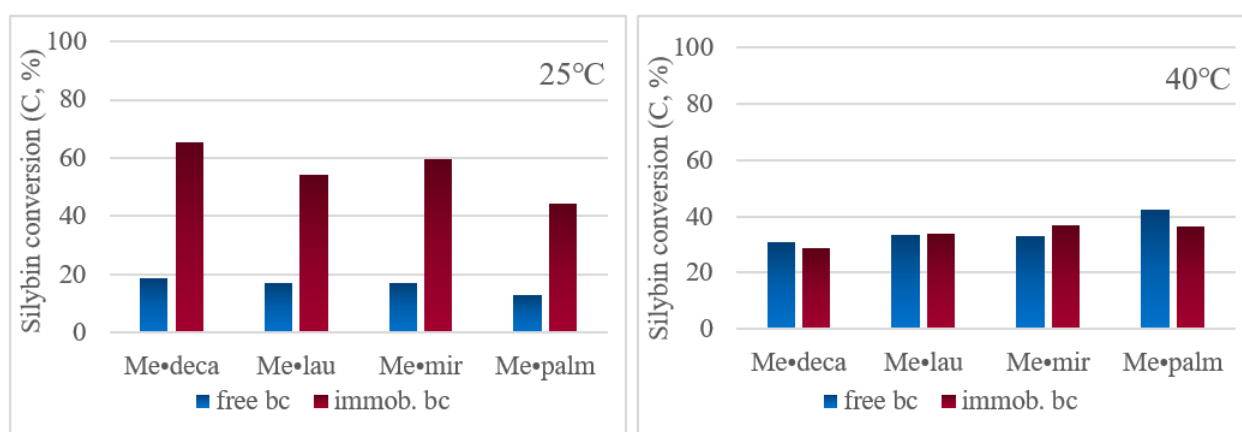


Figure 4. System performance in terms of silybin conversion by using different temperatures: 25 °C and 40 °C, with free lipase (■) or S5 biocatalyst (■). Experimental conditions: 2 mM Silybin A/B, 40 mM acylation reagent, 4.72 mg/mL free lipase/4.25 mg/mL S5 biocatalyst in 1 mL THF, at 25 °C or 40 °C and 1000 rpm for 24 h.

From the beginning, it is important to specify that the lipase fraction exhibited catalytic activity at 25 °C sustaining the cold-active character in the developed biocatalysts. For free lipase biocatalyst, the system performance was improved when the temperature increased from 25 to 40 °C. As an example, the silybin conversion was 19% for 25 °C and 31% for 40 °C using methyl decanoate for the acylation process. Therefore, increasing the temperature led to “an apparent” activation of the free lipase fraction.

Catalytic performance of the system was strongly improved when the immobilized lipase was used, especially at 25 °C. For the methyl decanoate agent, silybin conversion reached a maximum value of 65%, which is more than three times higher compared to the free lipase biocatalyst. Similar behavior was observed for all the methyl fatty acid esters tested. Therefore, the developed lipase fraction exhibited preponderantly cold-active catalytic activity in the immobilized forms.

The experiments were extended for all the prepared bio-composites (S1–5). Acylation of silybin was performed separately with different methyl fatty acid esters at 25 °C. The case of a free lipase biocatalyst was also chosen as a reference. The experimental results are presented in Figure 5.

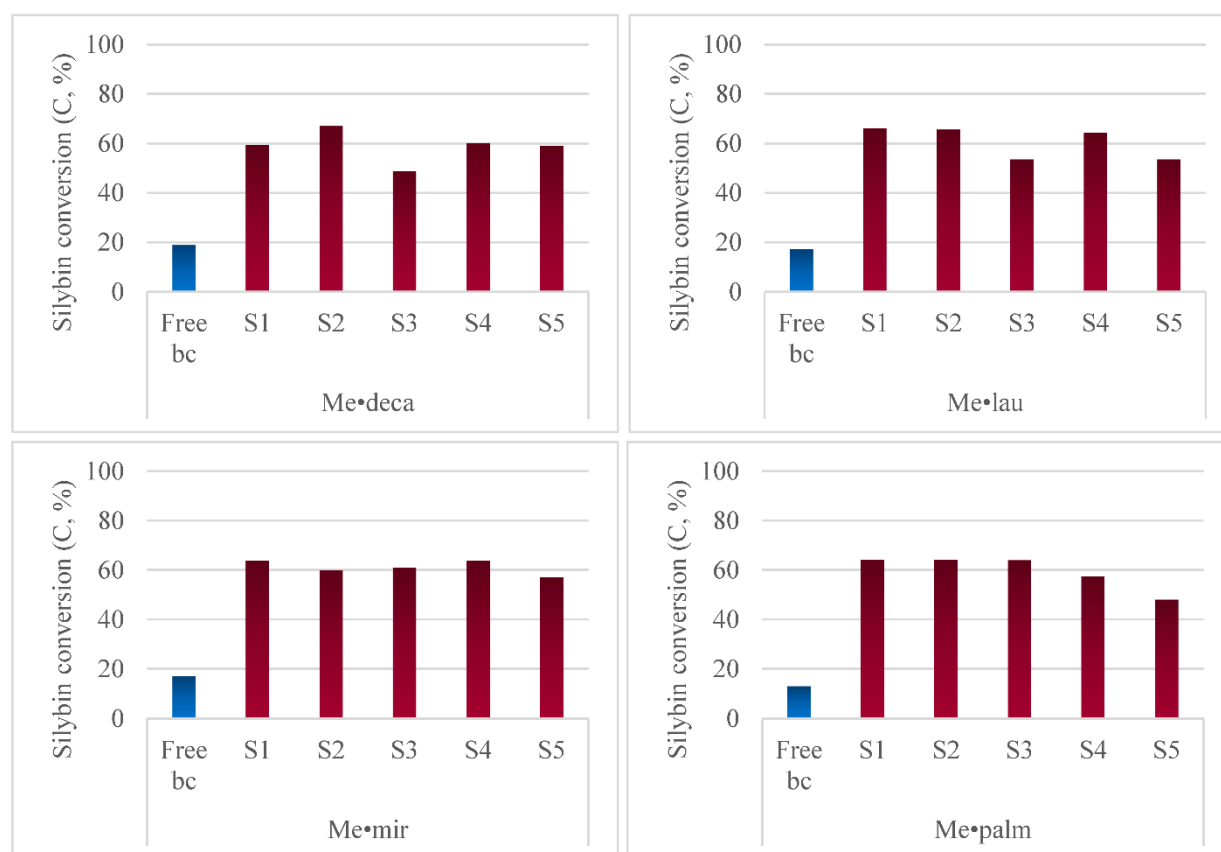


Figure 5. System performance in terms of silybin conversion for every biocatalyst specimen. Experimental conditions: 2 mM Silybin A/B, 45 mM Me-decanoate (Me•deca), 40 mM Me-laurate (Me•lau), 35 mM Me-miristate Me•mir), 30 mM Me-plamitate (Me•palm), 1:10 *v/v* biocatalyst, free (■) or immobilized (□), in 1 mL THF, at 25 °C and 1000 rpm for 24 h.

In the case of the free lipase specimen, the performance range in terms of substrate conversion varied between 13 and 19% (Figure 5). A slight variation in the silybin conversion with the hydrocarbon chain of the acylating agent was achieved, e.g., 19% for the methyl decanoate system and 13% for the methyl palmitate system. It is true that when the total protein content is embedded generically in the free biocatalyst, steric hindrances are a risky factor in achieving the synthesis, the lipase catalytic lid being restricted by the neighboring interactions.

For the immobilized lipase fraction, silybin conversion varied between 41 and 66% (Figure 5). The first important observation is based on catalytic activity improved up to 53% while comparing to the free enzyme. Thus, lipase is apparently activated by immobilization even though covalent attachment was performed. It has already been reported in the literature that lipases have such unusual behavior, but this is very rewarding when they are found at the interface between two different environments. Most studies are based on the hyper-activation phenomenon of lipases between organic and aqueous media [39,40]. However, the heterogeneity of the system given by the immobilized form and the liquid reaction medium was also reported as an alternative for lipase activation [41,42]. Now, our experimental results confirm again the lipase activation after immobilization on the solid support.

A second observation that correlated with the immobilized lipase biocatalysts (S1 and S3) is given by the increased biocatalytic potential in a constant trend with the increase in the hydrocarbon chain provided by the acylation agent. This behavior is obvious for the S3 bio-composite (49, 53, 61, and 64% silybin conversion for methyl decanoate, methyl laurate, methyl myristate, and methyl palmitate, respectively). Basically, the protein conformation

sustained by immobilization allowed the facial reception of the substrate at the catalytic site [43].

Moreover, the highest catalytic performance was recorded for the S2 biocatalyst and the lowest for S5, independently of the acylation agent. Maximum conversion of silybin (67%) was achieved for the S2 and methyl decanoate couple, while the minimum value (48%) was recorded for S5 and methyl palmitate. Therefore, the nano-scale biocatalyst (S2) offered a good catalytic performance in the developed system. This conclusion is also supported by the data from Tables 1 and 2.

3. Materials and Methods

3.1. Chemicals and Solutions

MES buffer (2-(N-morpholino) ethane sulfonic acid, 0.1 M stock solution, pH = 5), PBS buffer (phosphate buffered saline, 0.1 M stock solution, pH = 7.4) and TRIS-HCl buffer (2-Amino-2-(hydroxymethyl)-1,3-propanediol hydrochloride, 0.1 M stock solution, pH = 8) were standardly prepared. All the reagents used for the buffer preparation were purchased from Sigma-Aldrich (Taufkirchen, Germany).

For microbiological manipulations, R2B culture media were purchased from Melford Biolaboratories Ltd. (Ipswich, UK), while 1% Tween 80, 0.001% Rhodamine B, and 0.01% CaCl₂·2H₂O were from Sigma Aldrich-Merck, Darmstadt, Germany. The vegetal oils were achieved from commercial market and filtered before using.

For the biochemical methods were used acetone, ethanol, bovine serum albumin, *p*-nitrophenol and *p*-nitrophenyl butyrate, sodium bicarbonate, all purchased from Sigma Aldrich-Merk, Darmstadt, Germany. To build up the immobilized biocatalysts, 1-ethyl-3-(3-dimethylaminopropyl) carbodiimide, sodium periodate, glutaraldehyde, potassium bromide and sodium azide were purchased from Sigma-Aldrich Merck, Darmstadt, Germany, while the magnetic particles and amino-C₂-methacrylate type resin were purchased from Chemicell Company (Rostock, Germany) and Purolite Life Sciences Company (Wales, UK), respectively.

Acetone, acetonitrile, tetrahydrofuran of HPLC purity (99.99%), and reagents for the biocatalytic system comprising silybin A/B (silybin), methyl decanoate, methyl laurate, methyl myristate, and methyl palmitate, were obtained from Sigma-Aldrich Merck, Darmstadt, Germany.

3.2. Plate Screening Assays

Psychrobacter SC65A.3 strain was isolated from the perennial ice accumulated in Scarisoara Ice Cave (Romania) [26] and identified by 16S rRNA gene sequencing and genome sequencing (Macrogen, Seoul, Korea) (unpublished data). The strain was cultivated in R2B media at 15 °C for 3 days. For plate screening assays, 150 µL of culture in logarithmic phase growth [33] was used to inoculate R2A growth medium containing 1% Tween 80, and 0.01% CaCl₂·2H₂O or 1% olive/sunflower oils and 0.001% Rhodamine B. The plates were incubated at 15 °C for 3 days, and the presence of a lipolytic activity was evaluated by the specific products formed after hydrolysis: calcium oleate (as white precipitate) or fluorescent Rhodamine B-hydrolysate complex.

3.3. Preparation of the Protein Extract

Psychrobacter SC65A.3 was cultivated in R2B medium (500 mL) at 15 °C for 72 h, and the bacterial biomass was separated from the supernatant containing extracellular proteins by centrifugation at 4 °C for 20 min at 4800 rpm. The bacterial secreted proteins were precipitated with 80% acetone (2:1, *v/v* to culture medium) and recovered after centrifugation at 10,000 rpm for 10 min in 100 mM TRIS-HCl pH 8 [44]. The concentration of the resulted extracellular protein extract was measured spectrophotometrically at 280 nm by the BSA method [45].

3.4. Enzyme Assay

Lipase activity was measured by the colorimetric method [46], using *p*-nitrophenyl butyrate (*p*-NPB) as the substrate. The reaction mixture containing 2.5 mM *p*-NPB dissolved in ethanol, 1:4 *v/v* protein extract, and 32.5 mM Tris-HCl (pH 7.5) was incubated for 30 min at 25 °C or 37 °C, and the reaction was terminated by addition of 20 mM Na₂CO₃ blocking solution (10 min incubation). The activity was measured spectrophotometrically at 347 nm using 0.1–0.5 mM *p*-nitrophenol in ethanol as the calibration curve. The activity was expressed as μM/min/mg protein (units per mg of protein extract, where 1 U corresponds to μM product concentration obtained in 1 min). Kinetic parameters k_{cat} and K_m were calculated from substrate saturation curves carried out in the presence of 0.25–2.5 mM *p*-nitro phenylbutyrate substrate.

3.5. Lipase Immobilization

3.5.1. Preparation of the Immobilized Lipase Biocatalyst

The enzyme from the protein extract was attached to the solid support to improve the efficiency of the enzyme biocatalyst. For the immobilization, different approaches were applied based on covalent attachment of the enzyme via –NH₂ or –COOH residues. Magnetic particles and resin beads were considered as the solid support.

Covalent immobilization of the enzyme on the functionalized surface of magnetite particles was performed using the carbodiimide approach. The carbodiimide method involved the use of EDC (1-ethyl-3-(3-dimethylaminopropyl) carbodiimide, 0.25 M), PBS (0.1 M, pH = 7.4)/MES (0.1 M, pH = 5) washing buffers and blocking, and storage solution prepared in PBS with 0.1% bovine serum albumin and 0.05% sodium azide. Immobilization protocols were reproduced after the manufacturer's suggestions [47]. An amount of 1 mL of commercial suspension of Si-MAG-amine, Si-MAG-carboxyl, and fluid-MAG-ARA magnetic particles was gathered with a magnetic separator and foremost mixed with 0.25 M EDC in 0.1 M MES buffer (pH = 5). Then, 200 μL of protein extract was added and the resulting mixture was gently shaken for 2 h at room temperature.

For the NaIO₄ method, 500 μL protein extract was incubated in the dark with 5 mg NaIO₄ at room temperature for 30 min in the presence of Si-MAG-Hydrazine particles. The magnetic beads were placed to react with 0.25 mL of newly oxidized protein extract for 6 h at room temperature. PBS buffer (pH = 7) containing 0.1% BSA and 0.05% NaN₃ was used to block the ongoing reaction.

Covalent immobilization via glutaraldehyde (GA) linker was performed on amino-C₂-methacrylate type resin in MES buffer (10 mM, pH 5). The support, spherical beads of 150–300 μm diameter, was originally functionalized with –NH₂ groups using methacrylate crosslinker polymer. An amount of 0.1 g amino-C₂-methacrylate support was dispersed in the mixture containing 0.1% glutaraldehyde and 100 μL protein extract. After 2 h under gentle stirring, the immobilized enzyme was separated by centrifugation at 2000 rpm for 10 min. A washing step and resuspension were performed with/in PBS pH 7.4 buffer 3 times [48].

Finally, five different enzyme composites were obtained as indicated in Table 3:

Table 3. Immobilized lipase biocatalysts.

	Support	Immobilization Method
S1	sMP-COOH	EDC
S2	fMP-COOH	EDC
S3	sMP-NH ₂	EDC
S4	sMP-NH-NH ₂	NaIO ₄
S5	MTC-NH ₂	GA

3.5.2. Characterization of the Immobilized Lipase Biocatalyst

FTIR spectra of bio-composites and simple/functionalized supports were recorded using a Vertex 70 spectrophotometer (Bruker, Ettlingen, Germany) equipped with the Diffuse Reflectance Infrared Fourier Transform cell. A minimum amount of sample was diluted with potassium bromide matrix. Sixty-four scans were collected with a resolution of 4 cm^{-1} in the wavenumber range $4000\text{--}400\text{ cm}^{-1}$.

SEM micrographs were obtained through scanning electron microscopy, performed on a Jeol instrument (JSM-6610LV). Before SEM imaging, a thin layer of gold was dispersed over the sample in a high-vacuum chamber.

The activity of the immobilized lipase fraction was evaluated using the same protocol as for the free lipase fraction (see Section 3.4. Enzyme assay). The results of the colorimetric analysis (*p*-NPB protocol) allowed us to characterize the efficiency of the immobilization methods based on protein loading, recovery of lipase activity, and immobilization yield [49].

$$\text{protein loading (\%)} = \frac{m_i - m_s}{m_i} \times 100$$

$$\text{recovery of the lipase activity (\%)} = \frac{LA_{\text{immob}}}{LA_i} \times 100$$

$$\text{immobilization yield (\%)} = \frac{LA_i - LA_s}{LA_i} \times 100$$

m_i —initial protein amount (after concentration of the extracellular extract);

m_s —protein amount in the supernatant after immobilization step;

LA_{immob} —lipase activity of the immobilized protein fraction;

LA_i —lipase activity of the solution used for immobilization;

LA_s —lipase activity of the supernatant after immobilization.

3.6. Biocatalytic System for Silybin Acylation

Biocatalytic acylation of silybin was performed in a reaction phase with 2 mM silybin dissolved in THF and 45 mM Me-decanoate (Me•deca), 40 mM Me-laurate (Me•lau), 35 mM Me-miristate (Me•mir), or 30 mM Me-plamitate (Me•palm). The incubated mix of silybin with fatty esters was assisted by the lipase biocatalyst (10%, *v/v*) at 25 °C and 1000 rpm for 24 h. After reaction, the mixture was centrifuged for 15 min at 1500 rpm, allowing the separation of (free or immobilized) protein by collecting the supernatant separately. The supernatant was filtrated through 0.22 μm Millipore filters into HPLC vials and left in the oven at 70 °C for complete solvent evaporation. These dried samples were dissolved in the mobile phase of the HPLC-DAD system to finally reveal the sample content. For this, a 1260 Infinity HPLC modular system from Agilent Technologies was equipped with a Poroshell 120 EC-C18 column and a diode array-type detector (DAD). Analysis parameters implied the 1 mL/min flow rate mobile phase (41:59 = acetonitrile: acetone) and 25 μL injection volume. The signal was recorded at 210 nm for 30 min.

Using standards, identification of the sample components led to the following retention times: silybin at 2.4 min, methyl decanoate at 3.1 min, methyl laurate at 3.3 min, methyl myristate at 3.7 min, and methyl palmitate at 4.1 min. Silybin conversion was calculated based on the chromatographic data, by using the well-known formula:

$$\text{Conversion, } C (\%) = \frac{\text{mass of converted silybin}}{\text{initial mass of silybin}} \times 100$$

4. Conclusions

A valuable biocatalytic process based on the enzymatic activity of a cold-active lipase fraction was successfully elaborated for silymarin for improved bioavailability. A cold-active lipase fraction was obtained from a novel *Psychrobacter SC65A.3* strain isolated from Scarisoara Ice Cave (Romania). Enzyme immobilization allowed us to generate bio-

composites (S1–5) with preserved or even higher catalytic activity. Additionally, the kinetic parameters of the bio-composites sustained the cold-active character of the immobilized lipase biocatalysts (see S2 bio-composite) when measuring at 25 °C and 37 °C.

The developed biocatalytic process based on cold-active lipase activity involved the acylation of silybin as the main component of silymarin with methyl fatty acid esters (e.g., methyl decanoate, methyl laurate, methyl myristate, and methyl palmitate) for both free and immobilized (S1–5) biocatalysts. A maximum of 67% silybin conversion was reached for the S2 biocatalyst and methyl decanoate as the acylating agent.

This biocatalytic system could offer several advantages for silymarin valorization such as (i) energy saving by the cold-active behavior of the biocatalyst, (ii) derivatization of the silybin structure with fatty acid residue leading to a more hydrophobic product, (iii) curative features of silybin esters when omega acid residues are used as the acylation agent, and (iv) improving the efficiency of the cold-pressed milk thistle oil technology by considering the corresponding residues as a silybin and fatty acid source.

Supplementary Materials: The following are available online at <https://www.mdpi.com/article/10.3390/catal11111390/s1>, Figure S1: FTIR DRIFT spectra, Figure S2: SEM micrograph of *Aspergillus niger*.

Author Contributions: Conceptualization, G.R.G., C.P. and M.T.; methodology, G.R.G., V.I.P. (Vasile I. Parvulescu), S.N., G.-M.M. and M.E.; formal analysis, G.R.G., V.I.P. (Victoria Ioana Paun). and S.N.; investigation, G.R.G., V.I.P. (Victoria Ioana Paun) and G.-M.M.; data curation, G.R.G. and V.I.P. (Vasile I. Parvulescu); writing—original draft preparation, G.R.G. and M.T.; writing—review and editing, G.R.G. and M.T.; visualization, C.P.; supervision, M.T. and C.P.; project administration, M.T. and C.P.; funding acquisition, M.T. and C.P. All authors have read and agreed to the published version of the manuscript.

Funding: This research was funded by the UEFISCDI (Romania), grant number PN-III-P2-2.1-PED-2019-2461, 356PED/2020.

Data Availability Statement: The data presented in this study are available in the article and Supplementary Material.

Conflicts of Interest: The authors declare no conflict of interest.

References

1. Flora, K.; Hahn, M.; Rosen, H.; Benner, K. Milk Thistle (*Silybum marianum*) for the Therapy of Liver Disease. *Am. J. Gastroenterol.* **1998**, *93*, 139–143. [[CrossRef](#)]
2. Kuki, Á.; Nagy, L.; Deák, G.; Nagy, M.; Zsuga, M.; Kéki, S. Identification of Silymarin Constituents: An Improved HPLC–MS Method. *Chromatographia* **2011**, *75*, 175–180. [[CrossRef](#)]
3. Begum, S.A.; Sahai, M.; Ray, A.B. Non-conventional Lignans: Coumarinolignans, Flavonolignans, and Stilbenolignans. *Fortschr. Chem. Org. Nat.* **2010**, *93*, 1–70.
4. Csupor, D.; Csorba, A.; Hohmann, J. Recent advances in the analysis of flavonolignans of *Silybum marianum*. *J. Pharm. Biomed. Anal.* **2016**, *130*, 301–317. [[CrossRef](#)]
5. Vostálová, J.; Tinková, E.; Biedermann, D.; Kosina, P.; Ulrichová, J.; Svobodová, A.R. Skin Protective Activity of Silymarin and its Flavonolignans. *Molecules* **2019**, *24*, 1022. [[CrossRef](#)]
6. Bijak, M. Silybin, a Major Bioactive Component of Milk Thistle (*Silybum marianum* L. Gaertn.)—Chemistry, Bioavailability, and Metabolism. *Molecules* **2017**, *22*, 1942. [[CrossRef](#)] [[PubMed](#)]
7. Biedermann, D.; Vavříková, E.; Cvak, L.; Křen, V. Chemistry of silybin. *Nat. Prod. Rep.* **2014**, *31*, 1138–1157. [[CrossRef](#)]
8. Drouet, S.; Doussot, J.; Garros, L.; Mathiron, D.; Bassard, S.; Favre-Réguillon, A.; Molinié, R.; Lainé, É.; Hano, C. Selective Synthesis of 3-O-Palmitoyl-Silybin, a New-to-Nature Flavonolignan with Increased Protective Action against Oxidative Damages in Lipophilic Media. *Molecules* **2018**, *23*, 2594. [[CrossRef](#)]
9. Duan, L.; Carrier, D.J.; Clausen, E.C. Silymarin Extraction from Milk Thistle Using Hot Water. *Appl. Biochem. Biotechnol.* **2004**, *114*, 559–568. [[CrossRef](#)]
10. Theodosiou, E.; Purchartová, K.; Stamatis, H.; Kolisis, F.; Křen, V. Bioavailability of silymarin flavonolignans: Drug formulations and biotransformation. *Phytochem. Rev.* **2013**, *13*, 1–18. [[CrossRef](#)]
11. Duran, D.; Ötles, S.; Karasulu, E. Determination amount of silymarin and pharmaceutical products from milk thistle waste obtained from cold press. *Acta Pharm. Sci.* **2019**, *57*, 85. [[CrossRef](#)]

12. Fidrus, E.; Ujhelyi, Z.; Fehér, P.; Hegedűs, C.; Janka, E.A.; Paragh, G.; Vasas, G.; Bácskay, I.; Remenyik, É. Silymarin: Friend or Foe of UV Exposed Keratinocytes? *Molecules* **2019**, *24*, 1652. [[CrossRef](#)] [[PubMed](#)]
13. Hackett, E.S.; Twedt, D.C.; Gustafson, D.L. Milk Thistle and Its Derivative Compounds: A Review of Opportunities for Treatment of Liver Disease. *J. Vet. Intern. Med.* **2013**, *27*, 10–16. [[CrossRef](#)] [[PubMed](#)]
14. Di Costanzo, A.; Angelico, R. Formulation Strategies for Enhancing the Bioavailability of Silymarin: The State of the Art. *Molecules* **2019**, *24*, 2155. [[CrossRef](#)]
15. Di Fabio, G.; Zarrelli, A.; Romanucci, V.; Della Greca, M.; De Napoli, L.; Previtera, L. New Silybin Scaffold for Chemical Diversification: Synthesis of Novel 23-Phosphodiester Silybin Conjugates. *Synlett* **2012**, *24*, 45–48. [[CrossRef](#)]
16. Chambers, C.S.; Biedermann, D.; Valentová, K.; Petrásková, L.; Viktorová, J.; Kuzma, M.; Křen, V. Preparation of Retinoyl-Flavonolignan Hybrids and Their Antioxidant Properties. *Antioxidants* **2019**, *8*, 236. [[CrossRef](#)] [[PubMed](#)]
17. Kesharwani, S.S.; Jain, V.; Dey, S.; Sharma, S.; Mallya, P.; Kumar, V.A. An Overview of Advanced Formulation and Nanotechnology-based Approaches for Solubility and Bioavailability Enhancement of Silymarin. *J. Drug Deliv. Sci. Technol.* **2020**, *60*, 102021. [[CrossRef](#)]
18. Xanthakis, E.; Theodosiou, E.; Magkouta, S.; Stamatis, H.; Loutrari, H.; Roussos, C.; Kolis, F. Enzymatic transformation of flavonoids and terpenoids: Structural and functional diversity of the novel derivatives. *Pure Appl. Chem.* **2010**, *82*, 1–16. [[CrossRef](#)]
19. Vavříková, E.; Gavezzotti, P.; Purchartová, K.; Fuksová, K.; Biedermann, D.; Kuzma, M.; Riva, S.; Křen, V. Regioselective Alcoholysis of Silychristin Acetates Catalyzed by Lipases. *Int. J. Mol. Sci.* **2015**, *16*, 11983–11995. [[CrossRef](#)]
20. Brechley, J. Psychrophilic microorganisms and their cold-active enzymes. *J. Ind. Microbiol. Biotechnol.* **1996**, *17*, 432–437. [[CrossRef](#)]
21. Mangiagalli, M.; Brocca, S.; Orlando, M.; Lotti, M. The “cold revolution”. Present and future applications of cold-active enzymes and ice-binding proteins. *New Biotechnol.* **2020**, *55*, 5–11. [[CrossRef](#)] [[PubMed](#)]
22. Santiago, M.; Ramírez, C.; Zamora, R.; Parra, L.P. Discovery, Molecular Mechanisms, and Industrial Applications of Cold-Active Enzymes. *Front. Microbiol.* **2016**, *7*, 1408. [[CrossRef](#)] [[PubMed](#)]
23. Kavitha, M. Cold active lipases—An update. *Front. Life Sci.* **2016**, *9*, 226–238. [[CrossRef](#)]
24. Persoiu, A.; Lauritzen, S.E. Scarisoara Ice Cave. In *Ice Caves*, 1st ed.; Elsevier: Amsterdam, The Netherlands, 2018; Chapter 25.3.2.3, pp. 520–527.
25. Paun, V.I.; Lavin, P.; Chifiriuc, M.C.; Purcarea, C. First report on antibiotic resistance and antimicrobial activity of bacterial isolates from 13,000-year old cave ice core. *Sci. Rep.* **2021**, *11*, 54. [[CrossRef](#)] [[PubMed](#)]
26. Paun, V.I.; Icaza, G.; Lavin, P.; Marin, C.; Tudorache, A.; Perşoiu, A.; Dorador, C.; Purcarea, C. Total and Potentially Active Bacterial Communities Entrapped in a Late Glacial Through Holocene Ice Core From Scarisoara Ice Cave, Romania. *Front. Microbiol.* **2019**, *10*, 1193. [[CrossRef](#)]
27. de María, P.D.; Carboni-Oerlemans, C.; Tuin, B.; Bargeman, G.; van der Meer, A.; van Gemert, R. Biotechnological applications of *Candida antarctica* lipase A: State-of-the-art. *J. Mol. Catal. B Enzym.* **2005**, *37*, 36–46. [[CrossRef](#)]
28. Stergiou, P.-Y.; Foukis, A.; Filippou, M.; Koukouritaki, M.; Parapouli, M.; Theodorou, L.G.; Hatziloukas, E.; Afendra, A.; Pandey, A.; Papamichael, E.M. Advances in lipase-catalyzed esterification reactions. *Biotechnol. Adv.* **2013**, *31*, 1846–1859. [[CrossRef](#)]
29. Das, U.N. Essential fatty acids: Biochemistry, physiology and pathology. *Biotechnol. J.* **2006**, *1*, 420–439. [[CrossRef](#)]
30. Lawrence, G.D. *The Fats of Life. Essential Fatty Acids in Health and Disease*; Rutgers University Press: New Brunswick, NJ, USA, 2010; Chapter 2; pp. 15–20.
31. Gandhi, N.N.; Patil, N.S.; Sawant, S.B.; Joshi, J.B.; Wangikar, P.P.; Mukesh, D. Lipase-Catalyzed Esterification. *Catal. Rev.* **2000**, *42*, 439–480. [[CrossRef](#)]
32. Illanes, A. Chimosselective Esterification of Wood Sterols with Lipases. In *Enzyme Biocatalysis*; Springer: New York, NY, USA, 2008; Chapter 6.3; pp. 292–308.
33. Ramnath, L.; Sithole, B.; Govinden, R. Identification of lipolytic enzymes isolated from bacteria indigenous to Eucalyptus wood species for application in the pulping industry. *Biotechnol. Rep.* **2017**, *15*, 114–124. [[CrossRef](#)]
34. Peña, S.A.; Rios, N.S.; Carballares, D.; Sánchez, C.M.; Lokha, Y.; Gonçalves, L.R.B.; Fernandez-Lafuente, R. Effects of Enzyme Loading and Immobilization Conditions on the Catalytic Features of Lipase From *Pseudomonas fluorescens* Immobilized on Octyl-Agarose Beads. *Front. Bioeng. Biotechnol.* **2020**, *8*, 36. [[CrossRef](#)]
35. Barth, A. Infrared spectroscopy of proteins. *Biochim. Biophys. Acta (BBA) Bioenerg.* **2007**, *1767*, 1073–1101. [[CrossRef](#)]
36. Stoia, M.; Istrate, R.; Păcurariu, C. Investigation of magnetite nanoparticles stability in air by thermal analysis and FTIR spectroscopy. *J. Therm. Anal. Calorim.* **2016**, *125*, 1185–1198. [[CrossRef](#)]
37. Liu, X.; Guan, Y.; Shen, R.; Liu, H. Immobilization of lipase onto micron-size magnetic beads. *J. Chromatogr. B* **2005**, *822*, 91–97. [[CrossRef](#)]
38. Xu, Y.-Q.; Zhou, G.-W.; Wu, C.-C.; Li, T.-D.; Song, H.-B. Improving adsorption and activation of the lipase immobilized in amino-functionalized ordered mesoporous SBA-15. *Solid State Sci.* **2011**, *13*, 867–874. [[CrossRef](#)]
39. Rehm, S.; Trodler, P.; Pleiss, J. Solvent-induced lid opening in lipases: A molecular dynamics study. *Protein Sci.* **2010**, *19*, 2122–2130. [[CrossRef](#)] [[PubMed](#)]
40. Adlercreutz, P. Immobilisation and application of lipases in organic media. *Chem. Soc. Rev.* **2013**, *42*, 6406–6436. [[CrossRef](#)] [[PubMed](#)]

41. Sheldon, R.A.; van Pelt, S. Enzyme immobilisation in biocatalysis: Why, what and how. *Chem. Soc. Rev.* **2013**, *42*, 6223–6235. [[CrossRef](#)] [[PubMed](#)]
42. Bassi, J.J.; Todero, L.M.; Lage, F.A.; Khedy, G.I.; Ducas, J.D.; Custódio, A.P.; Pinto, M.A.; Mendes, A.A. Interfacial activation of lipases on hydrophobic support and application in the synthesis of a lubricant ester. *Int. J. Biol. Macromol.* **2016**, *92*, 900–909. [[CrossRef](#)] [[PubMed](#)]
43. Peña, S.A.; Rios, N.S.; Carballares, D.; Gonçalves, L.R.; Fernandez-Lafuente, R. Immobilization of lipases via interfacial activation on hydrophobic supports: Production of biocatalysts libraries by altering the immobilization conditions. *Catal. Today* **2021**, *362*, 130–140. [[CrossRef](#)]
44. Neagu, S.; Preda, S.; Anastasescu, C.; Zaharescu, M.; Enache, M.; Cojoc, R. The functionalization of silica and titanate nanostructures with halotolerant proteases. *Rev. Roum. Chim.* **2014**, *59*, 97–103.
45. Mach, H.; Middaugh, C.; Lewis, R.V. Statistical determination of the average values of the extinction coefficients of tryptophan and tyrosine in native proteins. *Anal. Biochem.* **1992**, *200*, 74–80. [[CrossRef](#)]
46. Moreno, M.D.L.; Garcia, M.T.; Ventosa, A.; Mellado, E. Characterization of *Salicola* sp. *â€¦*IC10, a lipase- and protease-producing extreme halophile. *FEMS Microbiol. Ecol.* **2009**, *68*, 59–71. [[CrossRef](#)] [[PubMed](#)]
47. Available online: <http://www.chemicell.com/home/index.html> (accessed on 14 November 2021).
48. Lite, C.; Ion, S.; Tudorache, M.; Zgura, I.; Galca, A.C.; Enache, M.; Maria, G.-M.; Parvulescu, V.I. Alternative lignopolymer-based composites useful as enhanced functionalized support for enzymes immobilization. *Catal. Today* **2020**, *379*, 222–229. [[CrossRef](#)]
49. Hill, A.; Karboune, S.; Mateo, C. Investigating and optimizing the immobilization of levansucrase for increased transfructosylation activity and thermal stability. *Process. Biochem.* **2017**, *61*, 63–72. [[CrossRef](#)]